Advanced Vehicle Control – Edelmann, Plöchl & Pfeffer (Eds)
© 2017 Taylor & Francis Group, London, ISBN 978-1-138-02992-7

Vehicle state estimation from a sports-car application point of view focusing on handling dynamics

Martin Haudum, Johannes Edelmann & Manfred Plöchl
Institute of Mechanics and Mechatronics, TU Wien, Austria

Manuel Höll
Dr. Ing. H.C. F. Porsche AG, Germany

ABSTRACT: Consistent vehicle states and parameters will become a requirement for the effective application of integrated vehicle dynamics control and automatic driving. Besides a basic model-based state estimation algorithm, additional modules, e.g. for the estimation of road grade and slope, and maximal longitudinal and lateral friction coefficients may decide on the quality of estimation when focusing on handling dynamics. Both enhanced complexity and inflexibility of a global vehicle state estimator and, alternatively, interdepended individual estimation modules face major drawbacks. This paper addresses a module based estimation approach to guarantee design flexibility, which has been tested with standard vehicle sensors at ordinary and extreme driving manoeuvres and road conditions to discuss benefits and drawbacks of the proposed modular vehicle state estimation approach.

1 INTRODUCTION

Vehicle state estimation has been given continuous interest and a large bulk of scientific papers has been published, e.g. (Wenzel et al. 2006, Antonov et al. 2011, Doumiati et al. 2013), in particular focusing on vehicle handling behaviour which is considered here only as well. A consistent set of vehicle states and parameters may in particular become important when benefits from integrated vehicle dynamics control methods shall be utilized, for either enhanced vehicle performance or active safety. An appropriate knowledge of the actual vehicle states, required to allow controllers for optimal performance and to decide about the best choice of controlled actuation devices, in combination with the estimation of varying parameters of the vehicle, vehicle–road contact and environmental conditions makes the estimation problem a comprehensive challenge. An overview of addressed estimation modules is given in Fig. 1. A focus will be set on "lateral dynamics", in particular on the estimation of the lateral velocities of the tyres, resp. of the centre of gravity of the vehicle. As this representative state variable (which is not sensed at production cars) is not only influenced by the driver's commands, but also derives from lateral road grade and depends on the available friction potential between tyres and road, also the modules "road grade" and "max. friction coefficients" will be addressed. Measurements have been performed with a 4WD sports-car, which is typically able to be vigorously operated at large vehicle accelerations and a large handling envelope can be utilized.

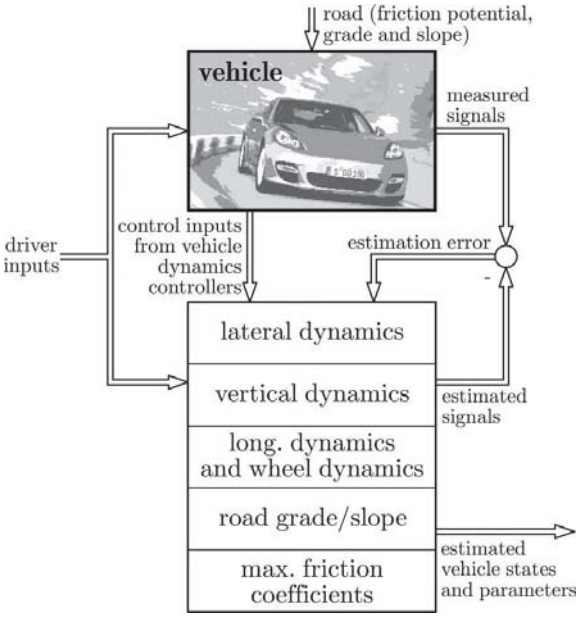

Figure 1. Overview of modular vehicle state/parameter observer.

The quality of estimated vehicle states is assessed w.r.t. the requirement of consistent levels of modelling complexity and demanded effectiveness of mentioned modules in their compound from a sports-car perspective, restricted by available sensors and signal quality, and limiting real-time and precision specifications.

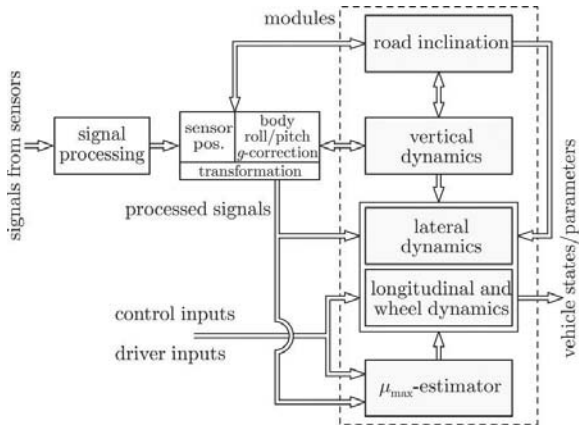

Figure 2. Signal flow corr. to Fig. 1.

The signal flow of the modular vehicle state/parameter observer is presented in Fig. 2 in more detail. Measured signals from CAN, such as steering angle, longitudinal and lateral acceleration, yaw rate, wheel speeds and engine torque, are pre-filtered, scaled, offset-aligned before they are transformed accounting for the sensor positions and portions of the gravitational acceleration g in the measured acceleration signals to finally become inputs to the various observer modules. Using basic CAN-signals only, mapping horizontal vehicle motion, does not allow to uniquely distinct effects from driver steering input, lateral road grade and lateral max. friction coefficient on vehicle side slip angle. For some kind of relief of this conflict, "mathematical" sensors are added to provide the steering rack force and inclination of the vehicle with respect to the inclined road using additional sensor inputs from the EPS and semi-active damping system. However, no roll rate sensor is available. For a stand-alone application of some modules, feedback loops shall be avoided, although only limited feasible.

2 VEHICLE AND TYRE MODEL

The vehicle and tyre model are kept as easy applicable (considering ECU restrictions, parametrization) and effective as possible, however, to account for an integrative vehicle dynamics controller environment, such as semi-active damping, rear wheel steering and active roll stabilization, respective input signals to the state observer need to be considered. Consequently, a 4-wheel vehicle model with respective force or steering angle actuation capabilities at the wheel centres and nonlinear tyre characteristics has been applied to be able to map longitudinal, lateral and vertical vehicle states for manoeuvres with large (combined) accelerations. The road surface may be inclined in longitudinal direction, road slope angle θ_R, and lateral direction, road bank/grade angle φ_R. Fig. 3 denotes main lateral vehicle states and parameters.

As a sports-car stands-out for its enlarged linear handling behaviour, Fig. 4, simplified models, such as the basic linear 2-wheel vehicle model and

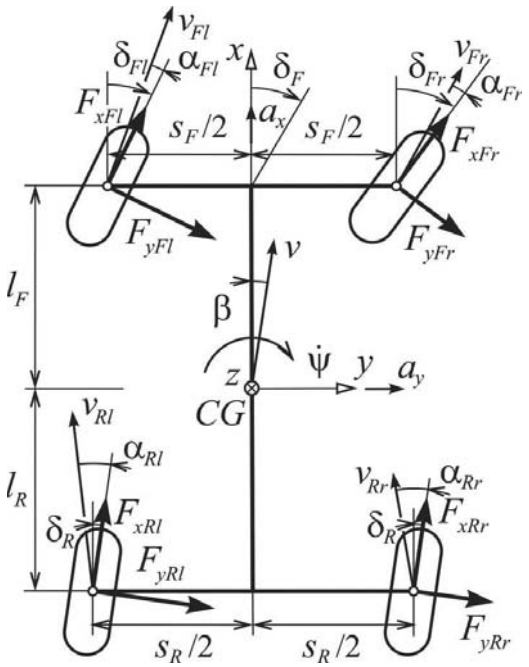

Figure 3. 4-wheel vehicle model (separate longitudinal and vertical model not depicted).

a nonlinear 2-wheel vehicle and tyre model, (1), (2), may be of interest due to its ease of application and parametrization as well. Estimation results derive from a (extended) Kalman filter, KF and EKF, respectively, see section 4. The Kalman filters build on the measured signals of the lateral acceleration and yaw rate (from CAN) in this case.

$$\dot{v}_y = \frac{1}{m}\left(F_{xR}\delta_R + F_{yR} + F_{xF}\sin\delta_F + F_{yF}\cos\delta_F\right) - g\cos\theta_R\sin\varphi_R - \dot{\psi}v_x \quad (1)$$

$$\ddot{\psi} = \frac{1}{I_z}\left(-l_R\left(F_{xR}\delta_R + F_{yR}\right) + l_F\left(F_{yF}\cos\delta_F + F_{xF}\sin\delta_F\right)\right) \quad (2)$$

Tyre models of different complexity have been considered/compared, in particular, a linear, exp-function based, brush and "Magic Formula" tyre model. While for the 4-wheel vehicle model combined longitudinal and lateral slip effects have been accounted for in the tyre model, the nonlinear 2-wheel vehicle model is based on lateral slip only. The following tests have been performed and simulated with a premium-class sports-car (mass about 2100 kg, wheel-base 3 m), here without 4WS. A modified brush tyre model has been applied. All three models have been individually parameterized, and do not descend from each other.

A comparison between the linear and the nonlinear vehicle model and measurements (from optical sensor and IMU) is illustrated in Fig. 5. As speed is usually moderate on an urban road, and steering angles may become quite large (here up to 400°), also side slip angles of the vehicle may reach a high level. Obviously, both vehicle models meet the measured vehicle side

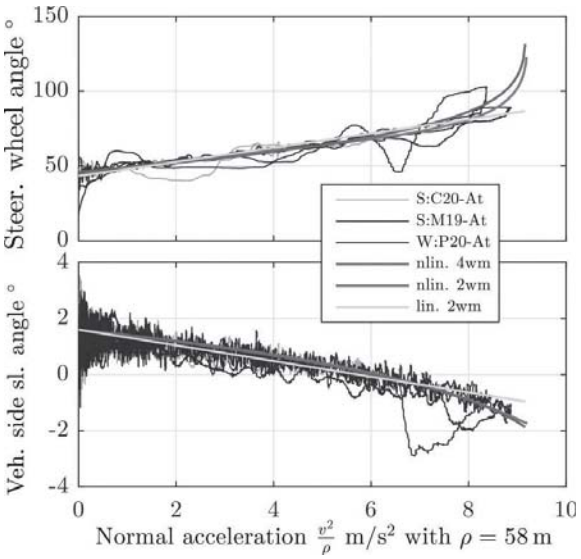

Figure 4. Handling diagram; measurements and model-based.

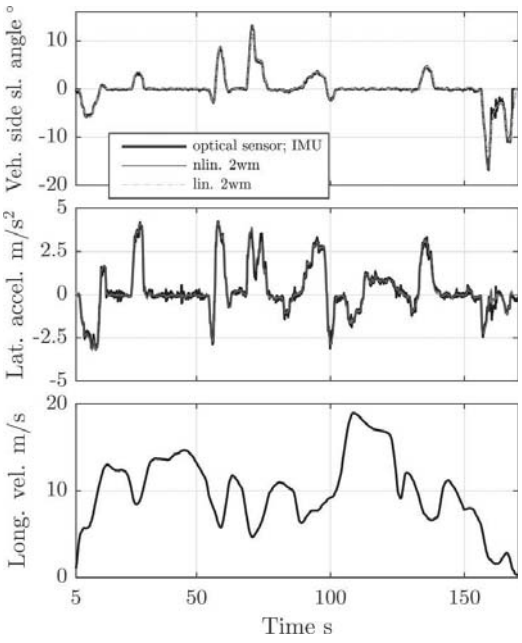

Figure 5. Urban road, model comparison.

slip angle (and lateral acceleration) very well, as lateral accelerations remain small.

Maintained step steer inputs have been carried out at about 50 km/h in Fig. 6. Lateral accelerations reach now a high level close to 10 m/s^2, and lateral tyre forces become saturated. Having the fit of the handling diagram in Fig. 4 in mind, it is no real surprise, that the linear model and the corresponding KF still meet quite well also the very high lateral accelerations. However, the match of the side slip angle of the vehicle becomes worse for increasing lateral accelerations before it completely fails. The results at (short) rather steady-state periods depend also on the fit of the steady-state handling diagram and the compromise between the fit of the lateral acceleration and vehicle

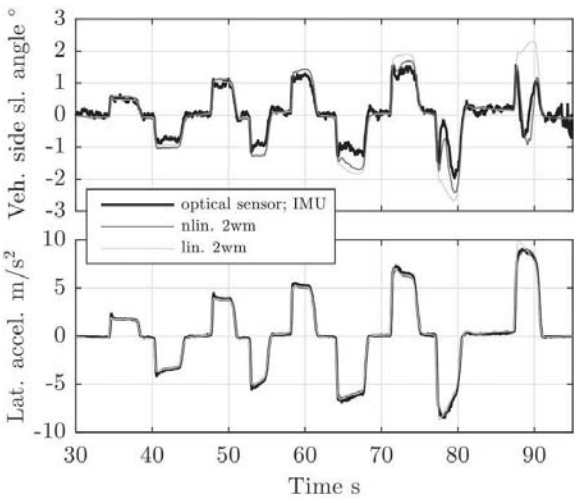

Figure 6. Maintained step steer manoeuvres, model comparison.

side slip angle. Here, the KF remains "inactive" as a good match of measured and estimated lateral accelerations already comes from the model parametrization. The shortcomings of the tyre model cannot be compensated with the KF, and the vehicle side slip angle may not be acceptable at severe driving manoeuvres. The nonlinear 2-wheel vehicle model reveals a less good fit of the vehicle side slip angle already in the handling diagram, Fig. 4, at small accelerations. The change of the vehicle side slip angle with time just before 90 s for constant measured lateral acceleration with constant steering angle but decreasing speed (changing the sign of the vehicle side slip angle), is qualitatively better mapped with the nonlinear tyre characteristics. A more detailed vehicle and tyre model may perform better, which will be addressed next.

A section of a race track is shown in Fig. 7. Pronounced braking and acceleration together with high lateral accelerations characterize this test. Here only the 4-wheel vehicle model including the dynamic change of load distribution and its enhanced tyre model accounts for the inaction between lateral tyre force and longitudinal slip of the 4WD vehicle. Consequently, wheel dynamics need to be included. Then, the match between estimated and measured vehicle states becomes promising up to the limits of tyre adhesion.

3 ROAD GRADE AND MAXIMUM FRICTION COEFFICIENTS ESTIMATION

The influence of lateral road grade and variation of road surface conditions will be discussed with respect to required and achieved accuracy of the parameter estimation module in particular related to resulting effects on the (lateral) state estimation module.

The estimation of the road bank angle φ_R is based on the kinematic relation for the total roll angle $\varphi_G = \varphi_G(\varphi_R, \varphi, \theta, \theta_R)$, for small angles $\varphi_G \approx \varphi_R + \varphi$,

$$a_{yMm} = \hat{\dot{v}}_{yM} + \dot{\psi}_m \hat{v}_{xM} + g \sin\varphi_G \cos\theta_G \,, \qquad (3)$$

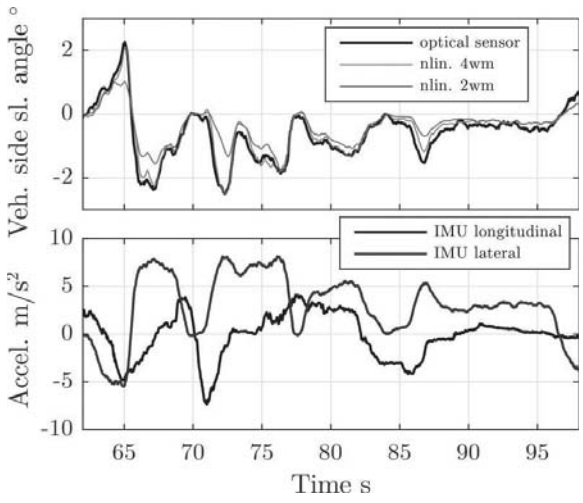

Figure 7. Race track, model comparison.

with measured yaw rate $\dot{\psi}_m$, lateral acceleration a_{yMm} in the vehicle body fixed reference frame at the location M of the sensor, and (small) roll and pitch angles, φ and θ, respectively. The longitudinal velocity $\hat{v}_{xM}$ is estimated independently in the "road slope" module considering a 4WD vehicle.

To avoid a feedback loop, the change of the lateral velocity in (3) with time cannot be used from the "lateral dynamics" module and is in general not available. Therefore, it is often neglected at all, and quasi steady-state manoeuvres are presumed. This assumption may fail when operating a sports-car with high dynamics, or when changing directions at large side slip angles of the vehicle.

A smart method to estimate a dynamic factor (DFC) of the manoeuvre directly related to $\hat{\dot{v}}_{yCG}$ is proposed in (Tseng 2000),

$$DFC = \frac{2\hat{v}_{xCG}^2}{l + \tilde{K}_{US}\hat{v}_{xCG}^2}\left(\tilde{K}_{US}a_{yCGm} + \frac{l}{\hat{v}_{xCG}}\dot{\psi}_m - \delta_F\right), \quad (4)$$

with understeer gradient $\tilde{K}_{US}$. The estimated road grade angle is scaled with $(1 - |DFC|/g)$, passing through the unscaled signal at steady-state, when the term in brackets and thus DFC become zero, which can easily be interpreted. For high dynamics the road grade angle tends to zero, which is correct on a horizontal road surface. The method is practicable if the change in lateral dynamics remains small.

For slowly changing $\hat{\dot{v}}_{yCG} = \hat{\dot{\beta}}\,\hat{v}_{xCG}$ and $\hat{v}_{xCG}$, the approximation

$$\hat{\dot{\beta}} = \frac{1 - \frac{ml_F\hat{v}_{xCG}^2}{C_{\alpha R}l_R l}}{1 + \frac{\hat{v}_{xCG}^2}{v_{\mathrm{ch}}^2}}\frac{l_R}{l}\dot{\delta}_F \quad \text{with} \quad v_{\mathrm{ch}}^2 = \frac{l}{\tilde{K}_{US}} \quad (5)$$

can be used (not considering small body roll and pitch here) to improve the estimation quality of the road grade angle φ_R and subsequently of the lateral vehicle states from the "lateral dynamics" module, although both road grade angle and vehicle side slip angle are not observable from a linear control theory point of view.

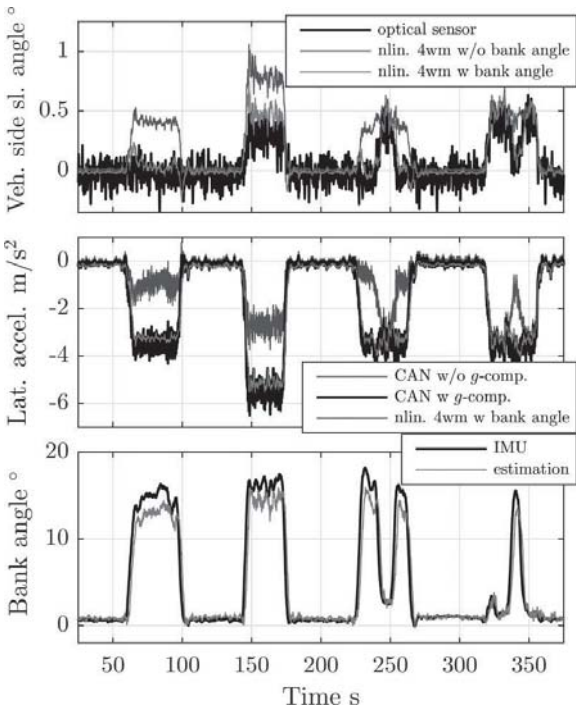

Figure 8. Lane change on banked turn (145 and 180 km/h).

The resulting signal is finally processed by a weighted complementary filter to better separate effects from high-frequency steering inputs from low-frequency road bank angle changes. In this way the bias in the acceleration signal from the gravitational acceleration on inclined roads may be removed to serve as input for the Kalman filter.

As an example, lane change manoeuvres on a banked road are shown in Fig. 8. Note the biased lateral acceleration of the CAN and the acceptable performance of the road bank angle estimator. Only then can reasonable estimates for vehicle states, here the vehicle side slip angle, be derived.

The tyre/road friction estimation module is based on utilizing effects of varied tyre/road friction on vehicle states, and is separated into longitudinal, lateral and combined excitation. Methods proposed in literature have been tested and most effective methods combined. A feedback loop from the "longitudinal and lateral dynamics" module has been avoided, and the module operates mostly autonomously. Here, friction estimation based on the Gough plot will be focussed with more details in e.g. (Pasterkamp and Pacejka 1997, Takagi and Inoue 2010, Matilainen and Tuononen 2011, Edelmann et al. 2015).

In the Gough plot, i.e. lateral tyre force over aligning torque, a pair of values (F_y, M_z) results in a unique pair of values $(\alpha, \mu_{\max})$. However, (F_y, M_z) are not available to directly estimate $\mu_{\max}$. Therefore, (F_y, M_z) derived with the tyre model of the 4-wheel vehicle model are transferred to a combined steering rack force $F_{\mathrm{tr\,sum}}$ incorporating front axle kinematics and load transfer,

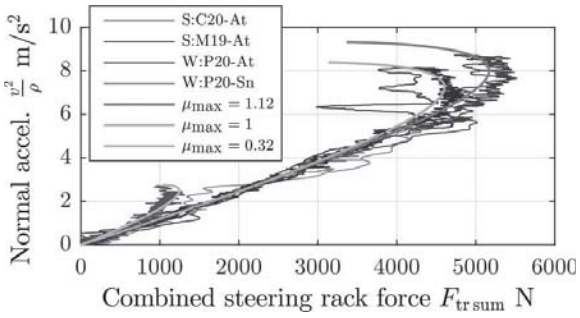

Figure 9. Combined steering rack force at steady-state cornering, corr. to Fig. 4.

see Fig. 9, for different friction levels (dry asphalt and ice). Where μ_{max}-lines almost coincide, the distinction between various friction levels becomes hard, also sensitivity to unknown or varying tyre/axle parameters is an issue. Nevertheless, the method is appealing due to its immediate guess of μ_{max}. Only a respective look-up table for $\mu_{max} = f(|a_y|, |F_{tr\,sum}|, |\delta_F|)$ has to be provided.

It is not clear then, how to incorporate μ_{max} of the "friction estimator" module to the EKF of the "lateral dynamics" module, where $\hat{\mu}_{max}$ is considered as a "constant" parameter (state) to be estimated. For example, μ_{max} from the friction estimator may be used as a trigger to adapt the covariance matrices of the EKF to allow for other consistent vehicle states. Or, some bounds with respect to μ_{max} may be introduced and a mathematical estimate projection ("clipping") method, (Simon 2006) applied to adapt $\hat{\mu}_{max}$ (and states) of the EKF within these bounds.

Fig. 10 illustrates the results of both methods. Initially $\mu_{max} = \hat{\mu}_{max}$ is set to 1 (dry road), then some arbitrary steering excitations on a road with snow on ice ($\mu_{max} \approx 0.36$) stimulate the friction estimator. Already after the first excitation μ_{max} immediately drops, but is "clipped" (close) to the upper bound until the third, litte stronger excitation. The first excitation peak is passed by the robust design of the **Q**-adaptation method, see section 4. When $\hat{\mu}_{max}$ is close to 0.36, even large vehicle side slip angles are estimated well. For low excitation, the influence of μ_{max} is not present, which becomes obvious during the first, and smallest steering excitation peak.

4 ESTIMATION ALGORITHM AND DESIGN

For state estimation a Kalman filter (KF) for the linear model and an extended Kalman filter (EKF) for the nonlinear models is used, (Gelb 1974, Simon 2006). Also an unscented Kalman filter (UKF) has be applied without much difference. Other estimation algorithms, such as a moving horizon estimator or sliding mode observer, have not be considered so far, and for specific manoeuvres some improvement might be expected. But in general, the EKF performs well over a wide range of manoeuvres and excitations.

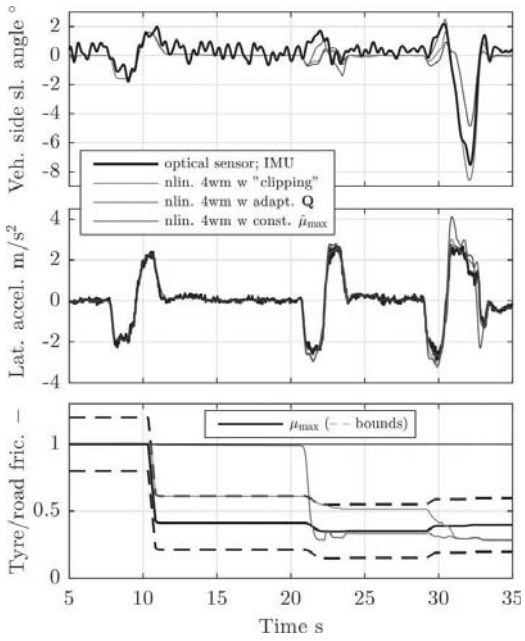

Figure 10. Combined estimation of friction potential and vehicle side slip angle.

Basically the design of a Kalman filter would be a straightforward task, which can be followed in many textbooks, (Gelb 1974, Simon 2006), if the underlying system model (equations, parameters and noise characterization) were exactly known. But in most cases, only the model equations and some of their parameters are available with sufficient accuracy. The characterization of process and measurement noise, more specifically the second order moments of noise – the covariance matrices of the process noise **Q** and measurement noise **R** – are (mostly) unknown. Therefore the elements of **Q** and **R** are often used as kind of tuning parameters in Kalman filter design.

Over five decades many papers have been published on the subject of Kalman filter design. In 1970 Mehra, (Mehra 1970, Mehra 1972), layed the foundation and classified the estimation of covariance matrices **Q** and **R** in four different categories: Bayesian estimation, e.g. (Matisko and Havlena 2013), maximum likelihood estimation, e.g. (Bavdekar et al. 2011), correlation methods, e.g. (Åkesson et al. 2008), and covariance matching methods, e.g. (Mohamed and Schwarz 1999). Further, classical system identification techniques, such as "subspace identification" (SID) or "time series methods", and all kinds of optimization approaches, e.g. (Powell 2002), shall be mentioned as well. Other effective design methods for the process noise covariance matrix, that exploits information about parametric uncertainties in the process model, when these are known, are given e.g. in (Schneider and Georgakis 2013).

However, irrespective of these mathematical approaches, **Q** and **R** are often determined by heuristic approaches, most commonly by "trial and error".

Some of the above approaches have been tested, but are not discussed here. For this paper, an optimization

method, (Powell 2002), applying a genetic algorithm, is applied to determine (only) the diagonal elements of **Q**. The objective function is based on the weighted squared estimation errors $\underline{e}^T\mathbf{W}\underline{e}$, provided that true-states are available (measured) for the tuning process. The problem with measurement noise in the true-states is roughly solved by offline (zero-phase) filtering. For the determination of **R** measured signals of steady-state manoeuvres have been assessed (covariance analysis of the measurement error).

A crucial aspect in KF-tuning is the choice of manoeuvres/input signals. From the mathematical point of view, already Mehra discusses this topic 1974 in (Mehra 1974). From a more practical point of view, a "wide excitation spectrum" shall be used, (Satria and Best 2002). Here measurements on a race track have been used.

5 CONCLUSIONS

It is reasonable to introduce individual modules for vehicle state and parameter estimation having flexibility and ease of design (for production development) in mind. However, adaptation of the modules to each other cannot be avoided, such as coordination of tyre characteristics to give an example. This results in a laborious task and requires a lot of testing to find out possible failures. In the end, a lateral dynamics, road grade and friction estimation module in combination can allow to reliably estimate vehicle states, such as the vehicle side slip angle, also at extreme handling manoeuvres with a sports-car with few failures.

The required model complexity is not as clear as expected. A Kalman filter can compensate deficiencies of the model, often with surprise to a large extent, even sometimes without much care about Kalman filter design parameters, but it can hardly be predicted at which manoeuvres the estimator may fail.

Due to the demanded linearity in the dynamic (handling) behaviour of a sports-car, a Kalman filter with a linear model already works quite well, if parameters are fitted well to steady-state cornering in particular, but may completely fail. The nonlinear 2-wheel vehicle model is effective also for large accelerations, if an appropriate tyre model is applied and reasonably parameterized. Lateral tyre force–side slip angle characteristics based on exp-functions are not appropriate for sports-car tyres, typically showing a long linear increase before a pronounced saturation. A more detailed 4-wheel vehicle model is required, if longitudinal dynamics need to be included, or respective vehicle dynamics control systems have to be mapped in the vehicle model. Additional modelled complexity has to be balanced with appropriate choice of covariance matrices of process (and measurement) noise. Experience in the choice of manoeuvres for Kalman filter design is essential to decide what kind of "wide excitation spectrum" is useful, which finally ends in trial-and-error, even though optimization methods have proven successful in the determination of covariance matrices of the Kalman filter.

To estimate vehicle states of a sports-car with 4WD on a banked race track or on icy roads is a tough challenge, but great to validate.

REFERENCES

Åkesson, B. M., J. B. Jørgensen, N. K. Poulsen, & S. B. Jørgensen (2008). A generalized autocovariance least-squares method for kalman filter tuning. *J. Process Contr. 18*, 769–779.

Antonov, S., A. Fehn, & A. Kugi (2011). Unscented kalman filter for vehicle state estimation. *Vehicle Syst. Dyn. 49*, 1497–1520.

Bavdekar, V. A., A. P. Deshpande, & S. C. Patwardhan (2011). Identification of process and measurement noise covariance for state and parameter estimation using extended kalman filter. *J. Process Contr. 21*, 585–601.

Doumiati, M., A. Charara, A. Victorino, & D. Lechner (2013). *Vehicle dynamics estimation using kalman filtering: experimental validation*. London, UK: John Wiley & Sons, Inc.

Edelmann, J., M. Gobbi, G. Mastinu, M. Plöchl, & G. Previati (2015). Friction estimation at tire–ground contact. *SAE Int. J. Commercial Vehicles 8*, 182–188.

Gelb, A. (1974). *Applied optimal estimation*. Cambridge (Massachusetts), USA: MIT press.

Matilainen, M. J. & A. J. Tuononen (2011). Tire friction potential estimation from measured tie rod forces. In *Intelligent Vehicles Symposium (IV), 2011 IEEE*, 320–325.

Matisko, P. & V. Havlena (2013). Noise covariance estimation for kalman filter tuning using bayesian approach and monte carlo. *Int. J. Adapt. Control 27*, 957–973.

Mehra, R. K. (1974). Optimal input signals for parameter estimation in dynamic systems–survey and new results. *IEEE T. Automat. Contr. 19*, 753–768.

Mehra, R. K. (1970). On the identification of variances and adaptive kalman filtering. *IEEE T. Automat. Contr. 15*, 175–184.

Mehra, R. K. (1972). Approaches to adaptive filtering. *IEEE T. Automat. Contr. 17*, 693–698.

Mohamed, A. H. & K. P. Schwarz (1999). Adaptive kalman filtering for ins/gps. *J. Geodesy 73*, 193–203.

Pasterkamp, W. R. & H. B. Pacejka (1997). The tyre as a sensor to estimate friction. *Vehicle Syst. Dyn. 27*, 409–422.

Powell, T. D. (2002). Automated tuning of an extended kalman filter using the downhill simplex algorithm. *J. Guid. Control Dynam. 25*, 901–908.

Satria, M. & M. C. Best (2002). Comparison between kalman filter and robust filter for vehicle handling dynamics state estimation. In *SAE Technical Paper 2002-01-1185*, 12 p.

Schneider, R. & C. Georgakis (2013). How to not make the extended kalman filter fail. *Ind. Eng. Chem. Res. 52*, 3354–3362.

Simon, D. (2006). *Optimal state estimation: Kalman, H infinity, and nonlinear approaches*. London, UK: John Wiley & Sons.

Takagi, F. & N. Inoue (2010). Estimation of maximum tire–road friction coefficient using electric power assist steering. *Mitsubishi Electric Advance 132*, 3 p.

Tseng, H. E. (2000). Dynamic estimation of road bank angle. In *AVEC'98*, Ann Arbor, USA, 421–428.

Wenzel, T. A., K. J. Burnham, M. V. Blundell, & R. A. Williams (2006). Dual extended kalman filter for vehicle state and parameter estimation. *Vehicle Syst. Dyn. 44*, 153–171.